Supplement to accompany J. Bourgeois & T.K. Pinegina

1997 Kronotsky earthquake and tsunami and their predecessors, Kamchatka, Russia

Earthquake and tsunami data

This supplement includes a reproduction of the original figure by Gusev (2004) of source regions for large Kamchatka earthquakes since 1899 (Fig. S1). In our paper, we use a revised version of this figure and discuss the bases for our suggested revisions.

Tsunamis have arrived to Kamchatka not only from local earthquakes but also from other regions, of which Kamchatka is particularly susceptible to tsunamis from Chile; Kamchatka is shadowed (protected) from non-local tsunamis originating in the North Pacific (Table S1; localities on Fig. S2). In order to interpret 20th century tsunami deposits in our field sites, we use these data to evaluate the possibility that at least one of the deposits is from a far-field event, Chile 1960.

Table S2 provides a summary of different researchers' assignments of moment magnitude, locations of mainshock epicenter and hypocenter, and centroid determinations for the December 1997 Kronotsky earthquake. There are some significant differences, which we discuss in our paper in terms of our documented evidence for tsunami runup averaging about 6 m along the coast north of Kronotsky Peninsula.

Figure S3 is a version of a previously published photo and sketch interpretation of 1997 Kronotsky tsunami effects on Kronotsky Cape (Pinegina et al., 2003).

The magnitudes of tsunamigenic and other large earthquakes originating along the Kamchatka subduction zone (and to its north) have been evaluated by Gusev and Shumilina (2004), with some suggested revisions to other catalogues (Table S3). One indicator of moment magnitude of earthquakes originating along the Kuril-Kamchatka subduction zone is their tide-gage amplitude in Hilo, Hawaii, as shown in Table S3 for all historical earthquakes and in Figure S4 for events with a tide-gage record in Hilo.

In A.D. 1923, there were two tsunamigenic earthquakes along the northern Kamchatka subduction zone. Table S4 is a compilation of information about those two tsunamis, which both affected Kamchatsky Bay. These observations and data help us evaluate which of these two tsunamis may have affected our field area in south Kamchatsky Bay.

Methodology for reconstructing paleoshorelines (Figure S5)

Many profiles show evidence of changes through time in beach-plain width and in surface elevation relative to sea level; that is, the shoreward, older parts of profiles are higher or lower than the seaward parts (Figure S5). Ideally, a reconstruction of the prehistoric coast and hence of paleotsunami size (runup and inundation as approximated by deposit extent) will include an estimate of horizontal shifts of shoreline location for paleo-inundation and an approximation of change in relative sea level for paleo- runup. We use tephra stratigraphy (as in Pinegina et al., 2013; MacInnes et al., 2016) and tephra mapping along profiles in order to reconstruct paleo-profiles. The reconstruction of the south Kamchatsky Bay profiles and their paleotsunamis was first performed and reported by Pinegina (2014).

Horizontal changes (Figure S5). We use the methods of Pinegina et al. (2013; also see MacInnes et al., 2016). These methods make an assumption that no widespread erosion has occurred, which is reasonable for the last 2000 years in south Kamchatsky Bay, but is a potential source of error. South Kamchatsky Bay profiles all indicate net progradation during the time interval examined. A tephra deposit is typically preserved in stratigraphy inland from the first dense vegetation (point *dv* on Figure S5) landward of the active (sandy) beach. Therefore, the seaward extent of a tephra in the stratigraphy (*dv1* or *dv3* in Figure S5) indicates the *dv* position at the time of eruption and ash deposition. Assuming today's active beach width is representative of the past, we

estimate the shoreline position at time "tephra x" to be the paleo *dv(x)* plus the modern active beach width. In general, our paleo- inundation estimates are minima because even though the beach-ridge plains are net progradational, short-lived periods of erosion can remove some of the accumulated coastal width. A general limitation to paleotsunami inundation reconstruction on a prograding shoreline is that estimates of maximum paleo- inundation will decrease back in time as the reconstructed beach plain width decreases. On the other hand, past erosion, which cannot be reconstructed, will result in an underestimate of beach plain width.

Vertical changes (Figure S5). In order to determine the change in land level relative to the sea, in each excavation we identify an elevation tied to sea level, for which we also use the point of the first growth of dense vegetation (*dv*, Figure S5). We measure and mark this point on our modern profiles and associate this point in excavations with good preservation of volcanic ash layers (tephra). The limit of dense vegetation approximates the swash limit and storm high tide, seaward of which tephra will rarely be preserved. Dense vegetation (primarily dune grass, *Elymus* sp.) grows only on the part of the profile that is rarely affected by storms, except for some washover, and thus soil-tephra cover begins to form on these surfaces. Net uplift or subsidence is the difference between the modern *dv* elevation and the paleo *dv* elevation (Figure S5). A general limit to paleotsunami runup estimates for the case of uplifting coastlines is that maximum paleo- runup will decrease back in time as the reconstructions bring paleo- profiles downward.

Historical and paleotsunami data, including excavation elevations and distances from shoreline

Herein we summarize graphically the data on which our paleotsunami analysis is based. These data were first synthesized by Pinegina (2014) for many localities along the Pacific coast of Kamchatka. In this supplement, we include data from Ust-Kamchatsk (Pinegina et al. 2012; Pinegina 2014) because it is within (at the north end of) Kamchatsky Bay (Fig. S2).

The distribution of elevations (meters above sea level) and distances (meters from modern shoreline) of excavations in the field area, southern Kamchatsky Bay, are shown in Figure S6. We use these distances and elevations for reconstructing tsunami sediment runup and inundation for 20$^{\text{th}}$ century tsunami deposits (Fig. S7). For south Kamchatsky Bay, the maximum profile width is less than 800 m; in north Kamchatsky Bay, distances reach about 1.8 km (Figs. S7, S8).

The elevation and distance of tsunami deposits above KS$_{1907}$, including data from the Ust-Kamchatsk area, north Kamchatsky Bay, are shown in Figure S7. Some excavations contain no deposits above KS$_{1907}$. The deposit that is present in the most excavations we interpret as from 1923; the second-most extensive deposit is from 1997. Rarely there is a third deposit between the other two, which we assign to 1960 Chile.

The number of paleotsunami deposits per tephra interval for three intervals below KS$_{1907}$ are shown in Figure S8, which includes data from north Kamchatsky Bay near Ust-Kamchatsk. For each interval, the elevation and distance from shoreline of each excavation is reconstructed using methods as in Figure S5.

Locations of the 5 December 1997 Kronotsky earthquake rupture, according to different studies

Our tsunami-deposit study has implications for the rupture zone of the 1997 Kronotsky earthquake. Figure S9 is a compilation of several different models for the location of this rupture zone, from previously published work.

Table S1. HISTORICAL TSUNAMIS AFFECTING (or possibly affecting) THE KAMCHATSKIY BAY COAST OF KAMCHATKA*

EARTHQUAKE PARAMETERS			RECORDS OF TSUNAMI RUNUP (*tide gage records in italics*) in meters									
			Locations South to North Olga Bay to Bering Island								MAX KAM	Hilo, HI
Date (local)	Source region	Mw	Olga Bay	Kron. Cape	CHAZHMA ADR-BIST	Shuber-tovo	south of U-K	*U-K tide gage*	Kamch River	Bering I. (south)		
5-Dec-97	Kronotskiy Peninsula	7.8/7.9^	0.5-1	1.5	this paper			*not working*		*incompl record*	this paper	*0.24*
8-May-86	Andreanof Islands#	8						*0.04*		*0.09*	*0.09*	*0.28*
4-Mar-85	Chile	7.7						*0.03*				*0.77*
28-Dec-84	Kamchatsky Strait	7						*0.02*		*0.17*		
18-Aug-83	Kamchatsky Bay	6.8						*0.02*				
15-Dec-71	Commander Is.	7.8^						*0.47*				*0.10*
23-Nov-69	Bering Sea	7.7						*0.2*			10-15	*0.10*
04-Feb-65	w. Aleutians	8.7			only recorded on Petropavlovsk tide gage						*0.08*	*0.30*
28-Mar-64	Alaskan Peninsula	9.2			only recorded on Petropavlovsk tide gage						*0.06*	~3
24-May-60	Chile	9.5	4				3	*0.8*	3-4	3-3.5	7	~10
05-Nov-52	s. Kamchatka	9	10-13			0.5-1		*0.1*		2	10-15	*1.1*
02-Apr-46	Aleutians	8.1		no record on Kamchatka 0.1-0.2 in northern Japan, max 1.1 in Japan						—	~9
14-Apr-23	Kamchatskiy Bay	7.3/8.2^					20-30		11	4	20-30	*0.30*
04-Feb-23	Kronotskiy Bay	8.5^	4-5 km up river		4-5 km up Chazhma R.				3		6-8	6.10
17 May 1841	s. Kamchatka	9^									15	4.6
August 1792	Avachinsky Bay to n. Kamchatsky Bay	8.25**										
15 Apr 1791	Kamchatskiy Bay	(7.5)^						effects 7 km upstream				—
4 Nov 1737	N Kamchatskiy Bay	(7.8)^										
17 Oct 1737	s. Kamchatka	9.2^									>30?	—

*Primary sources: Zayakin and Luchinina, 1987; NEIC (formerly NGDC) Natural Hazards Data, online

^Kamchatka Mw's from Gusev and Shumilina, 2004; G&S 8.2 for 14Apr23 is based on tsunami; see text discussion

#Andreanof Islands, 1996, 7.9; 1957, 8.6, no catalogue observations for Russia

**Ms from Zayakin & Luchinina

Table S2. Epicentral locations, centroids and moment magnitudes for the 5 December 1997 Kronotsky earthquake (ISC* Event 1056468 "Near east coast of Kamchatka Peninsula")

Origin of analysis	ISC*origin ID	Lat °N	Long °E	Moment/Mw	Additional information
Epicenter/Mainshock^					
KEMSD GS RAS		54.95	163.23		Gusev et al. 1998, Luneva&Lee 2003
Zobin& Levina 2001; Slavina et al. 2007		54.64	162.58		Kamchatka network catalogue; S&al 162.55
KRSC reported in ISC database	2296136	54.64	162.55		ISC KRSC = KEMSD
ISC--International Seismological Centre	1056468	54.8043	162.0069		accessed online 13 Mar 2017
Engdahl and Villsenor 2002	2329842	54.797	162.003		ISC-CENT--Centennial Catalogue
EHB — reported in ISC online	9258772	54.792	162.001		ISC — Engdahl, vonderHilst & Buland, 1998
NAO — reported in ISC online	2296140	55	162		ISC — NORSAR, Norway
EIDC — Arlington, VA	2296135	54.8523	161.9921		ISC—Experim. (GSETT3) Internatl Data Ctr
BJI — China	2296137	54.82	161.90		ISC — China Earthquake Administration
Centroid/Moment Tensor solutions & models					
Geophys Survey Russian Academy Sci.	2296139	54.881	161.947	2.2×10^{20}Nm	ISC — MOS, Obninsk
NEIC, Golden, CO [USGS]	2296138, 5159529	54.841	162.035	4.1×10^{20}Nm	ISC; National Earthquake Information Center
Global CMT [formerly Harvard]	2296141	54.31	161.91	7.8	ISC - HRVD, Global GMT #120597C
Harvard CMT early		54.08	162.29	7.9	reported in Gusev et al., 1998
Sohn, 1998		54.8	162	uses 2.5×10^{20}Nm	model from tsunami analysis; location approx.
Burgmann et al, 2001		54.19#	162.57#	uses 3.8×10^{20}Nm	acos model based on GPS data
Burgmann et al, 2001		54.23#	162.33#	uses 4.1×10^{20}Nm	bcos model based on GPS data

*ISC = International Seismological Centre, *On-line Bulletin* , http://www.isc.ac.uk, Internatl. Seismol. Cent., Thatcham, United Kingdom, 2014; last accessed 20 March 2017

^Ordered by longitude, easternmost to westernmost

#Latitude and longitude refer to the center of the upper dislocation edge of the modeled centroid

Table S3: Historical tsunamigenic events in the Kuril-Kamchatka region and their record in Hilo, Hawaii

Date (young to old)			Location epicenter/rupture		Earthquake		Tsunami runup/tide			COMMENTS
Year	Mo	Day	Latitude °N	Region	M NCEI	Mw^	Runup max m	Hilo tide m	Hilo runup m	
2009	1	15	46.857	Central Kuril Is.	7.4	~	*	0		0.11 m tide gage Severo Kurilsk
2007	1	13	46.243	Central Kuril Is.	8	~	6-20**	0.11		outer rise event
2006	11	15	46.592	Central Kuril Is.	8.3	~	6-20**	0.475		
1997	12	5	54.88	Kamchatka	7.8	7.9	(9)	0.24		(runup max from deposits)
1995	12	3	44.663	S. Kuril Is.	7.9	~	*	0.228		
1994	10	4	43.773	Shikotan Is.	8.3	~	10.4	0.16		outer rise event
1993	6	8	51.25	S. Kamchatka	7.5	7.5	*	0.06		
1971	12	15	55.91	N. Kamchatka	7.8	7.8	(13)	0.1		0.47 on Ust' Kamch. tide gage; (runup max from deposits)
1969	11	22	57.8	N. Kamchatka	7.7	7.7	15	0.1		
1963	10	13	44.81	S. Kuril Is.	8.5	~	4.5	0.4		
1963	10	20	44.1	S. Kuril Is.	6.7	~	15	0.1		
1959	5	4	53.9	Kamchatka	8.2	8	1.5-2	0.1 [#]		
1958	11	6	44.53	S. Kuril Is.	8.3	~	5	0.2		limited nearfield obs, 5 m on Shikotan
1958	11	12	44.2	S. Kuril Is.	7	~	1	0.1		
1952	11	4	52.3	Kamchatka-Kuril	9	9	(20)	1.1	3.4	(runup max from deposits)
1933	1	8	49.12	N. Kuril Is.	na	na	9	0		Kharimkotan landslide
1927	12	28	53.8	Kamchatka	7.3	7.5	*	0.1		
1923	4	13	55.4	N. Kamchatka	7.3	8.2	14	0.3		
1923	2	2	52.5	Kamchatka	8.3	8.5	8		6.1	
1918	9	7	45.5	S. Kuril Is.	8.2	~	12		1.5	
1917	1	30	55.2	N. Kamchatka		8	*			no tsunami; strike-slip event, Steller f.z.
1841	5	17	52.5	Kamchatka	8.4	9	15		4.6	
1737	10	17	50.5	S. Kamchatka		9.2	30?			
1737	11	4	55.5	N. Kamchatka		7.8	*			

Primary sources: Zayakin and Luchinina, 1987; NCEI Tsunami database

*no nearfield data

^from Gusev & Shumilina, 2004

[#]1959 measurement is from Honolulu

**2006 and 2007 runup could not be definitely distinguished in post-tsunami survey

Table S4. Comparison of measurements and observations, 1923 Kamchatka tsunamis

Observation locality	Latitude	Longitude	3 Feb 1923		13 April 1923	
			Runup (m)	type	Runup (m)	type
Bering Island, Commander Islands	55.20	166.01			4	1
Kamchatka Pacific coast, north to south						
Dembi Spit area, east Ust Kamchatsk	56.22	162.52			11	1
Kamchatka River	56.25	162.44			broke ice 7 km upriver	1
Tsutsumi fish plant	55.176	162.313	damaged cabin on first ridge*	1	4 km inundation** ext. damage	1
First River, north central Kamch Bay	56.05	162.05			20	1
Chazhma River, south Kamch Bay	55.06	161.82	4-5 km upriver	1		
Semyachik, central Kronotsky Bay	54.12	159.98	6	1		
Kolygir Bay, Shipunsky Peninsula	53.42	159.85	8	1		
Ostrovnoye, north Avachinsky Bay	53.25	159.57	obs	1		
Nalychevo R. north Avachinsky Bay	53.16	159.24	obs	1		
Khalaktirka, central Avachinsky Bay	52.98	158.83	8.4^	^		
Avachinsky Gulf (interior)	52.97	158.50	obs	1		
Japan Pacific coast, north to south						
Hanasaki, Hokkaido	43.278	145.568	*0.23*	*2*	*0.07*	*2*
Ayukawa, Miyagi, Japan	38.300	141.500	*0.33*	*2*	*0.17*	*2*
Kushimoto, Wakayama, Japan	33.467	135.783	*0.5*	*2*		
Hososhima, Miyazaki, Japan	32.433	131.667	*0.2*	*2*		
Pacific islands						
Hilo, Hawaii, HI, USA	19.733	-155.067	6.1	1	*0.3*	*2*
Kahului, Maui, HI, USA	20.895	-156.477	3.5	1		
Honolulu, Oahu, HI, USA	21.307	-157.867	*0.9*	*2*	*0.2*	*2*
Haleiva, Oahu, HI, USA	21.593	-158.106	3.7	1		
Apia, Upolu Is, Samoa	-13.827	-171.761	obs	*2*		
West coast North America. north to south						
Tofino, BC, Canada	49.153	-125.913	*0.14*	*2*	*0.08*	*2*
San Francisco, CA, USA	37.807	-122.465	*0.1*	*2*	*0.15*	*2*
Santa Cruz, CA, USA	36.970	-122.020	obs	1		
Los Angeles, CA, USA	33.717	-118.267	obs	1		
San Diego, CA, USA	32.715	-117.174	*0.2*	*2*	*0.1*	*2*

Primary source: for Kamchatka: Zayakin and Luchinina; remainder: NCEI catalogue

Type: 1 = runup, elevation above sea level; *2 = tide gage amplitude*

*first beach ridge ~3.5 m above sea level; second ~4 m asl (profile in Pinegina et al., 2014)

**inundation may have been via river to lagoonal areas between ridges; sediment inundation 1 km (Pinegina et al., 2012)

^based on deposits, Pinegina and Bazanova, 2016
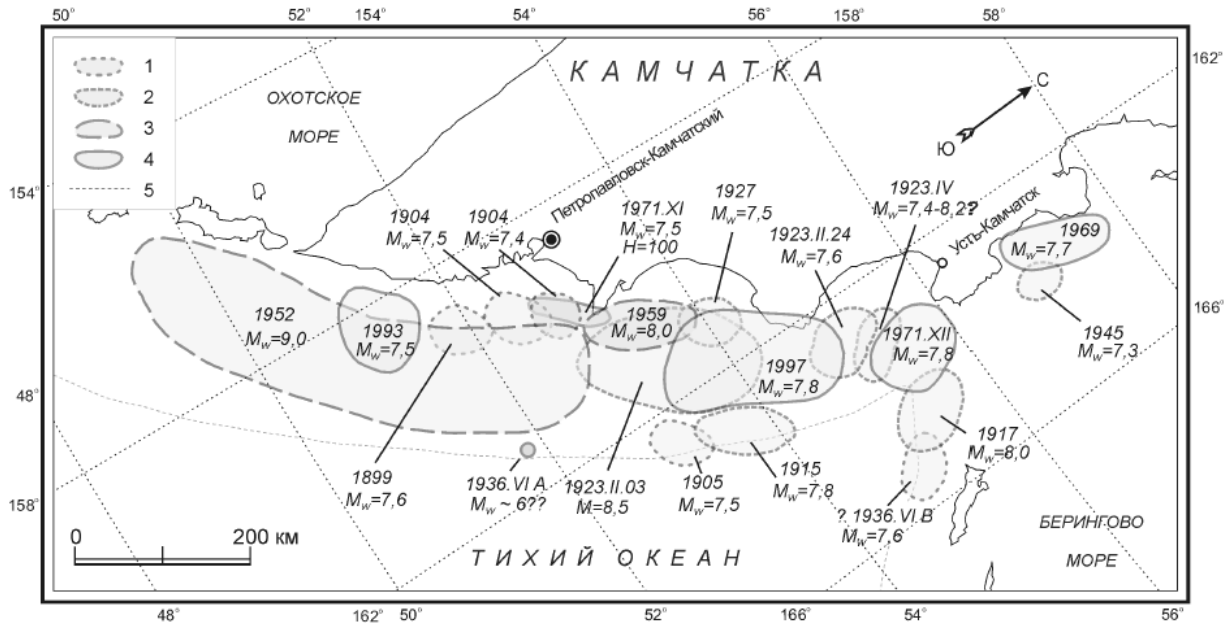
Рис. 1. Новый вариант расположения очаговых зон землетрясений Камчатки за 1899-2003 гг.

Figure S1. Original figure from which we make comments and suggested revisions in the text (Gusev, 2004; used with permission) Translated caption: "New version (of) source location zones of Kamchatka earthquakes 1899 to 2003." Also see Gusev and Shumilina (2004).
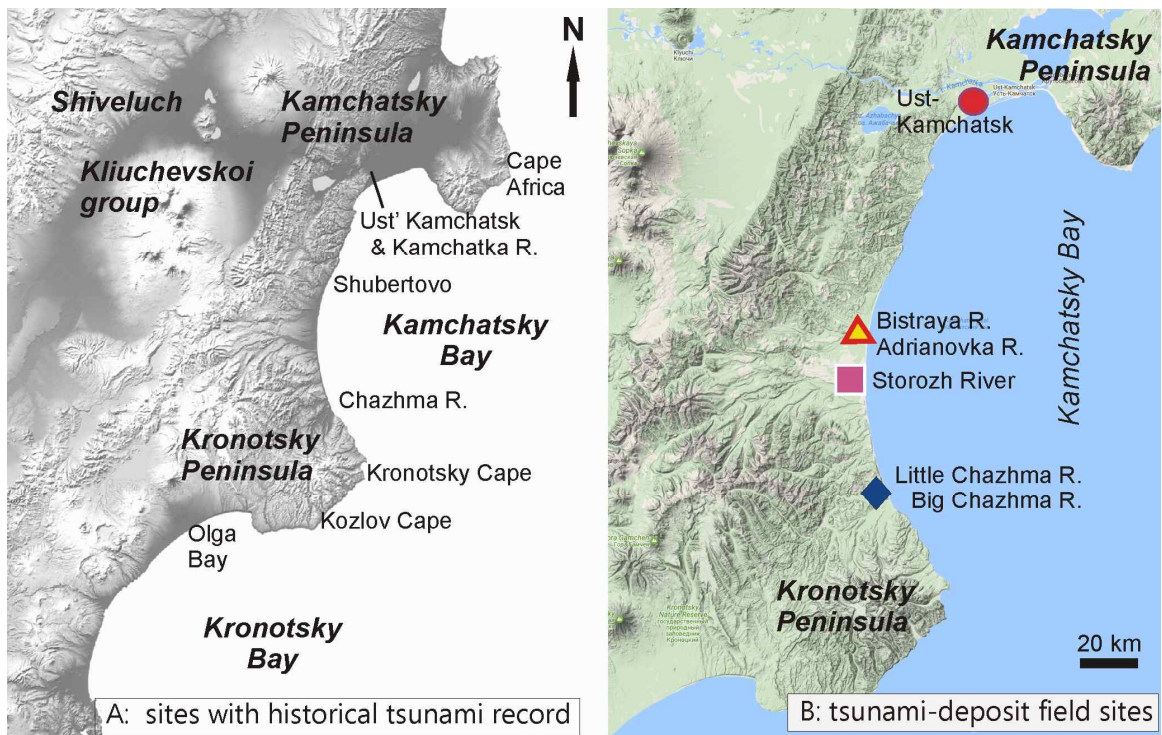
Figure S2. Left: sites in the field region with historical tsunami records, shown in Table S1. **Right:** field sites in south Kamchatsky Bay as well as location of Ust Kamchatsk field site (Pinegina et al. 2012; Pinegina, 2014) with data displayed in following figures.
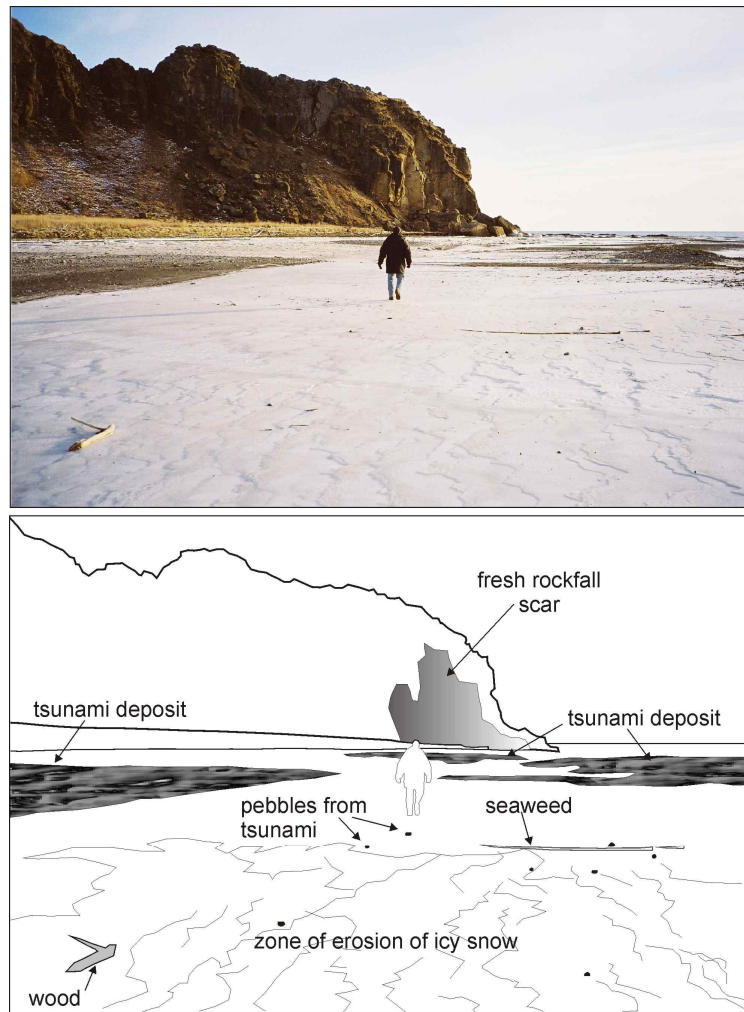
Figure S3. View of Kronotsky Cape during 9 December 1997 post-earthquake and post-tsunami survey, with sketch to label features; photo T. Pinegina. Modified from Pinegina et al. (2003).
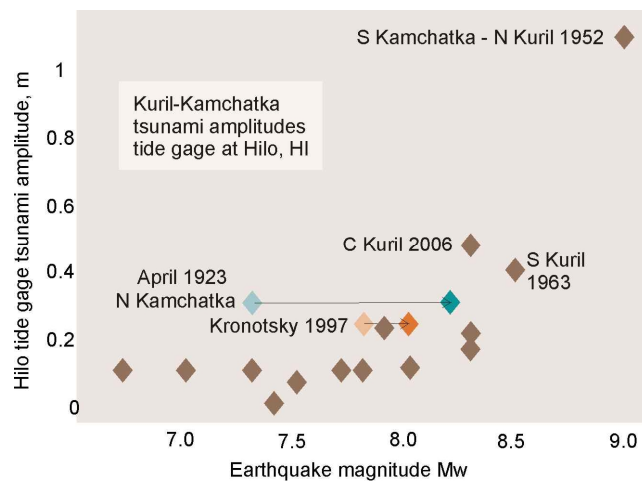
Figure S4. Tsunamigenic earthquakes from Kuril-Kamchatka subduction zone and their Hilo tide gage amplitude. Plotted from data in Table S3. April 1923 earthquake is reinterpreted by Gusev and Shumilina (2004) to be a magnitude 8.2 (see Fig. S2), plotted as darker blue. Kronotsky 1997 is plotted in light tan at 7.8 and dark tan as 8.0, which fits the tide-gage trend better, but not so convincingly as the 1923 April revision. "C Kuril" – Central Kuril.
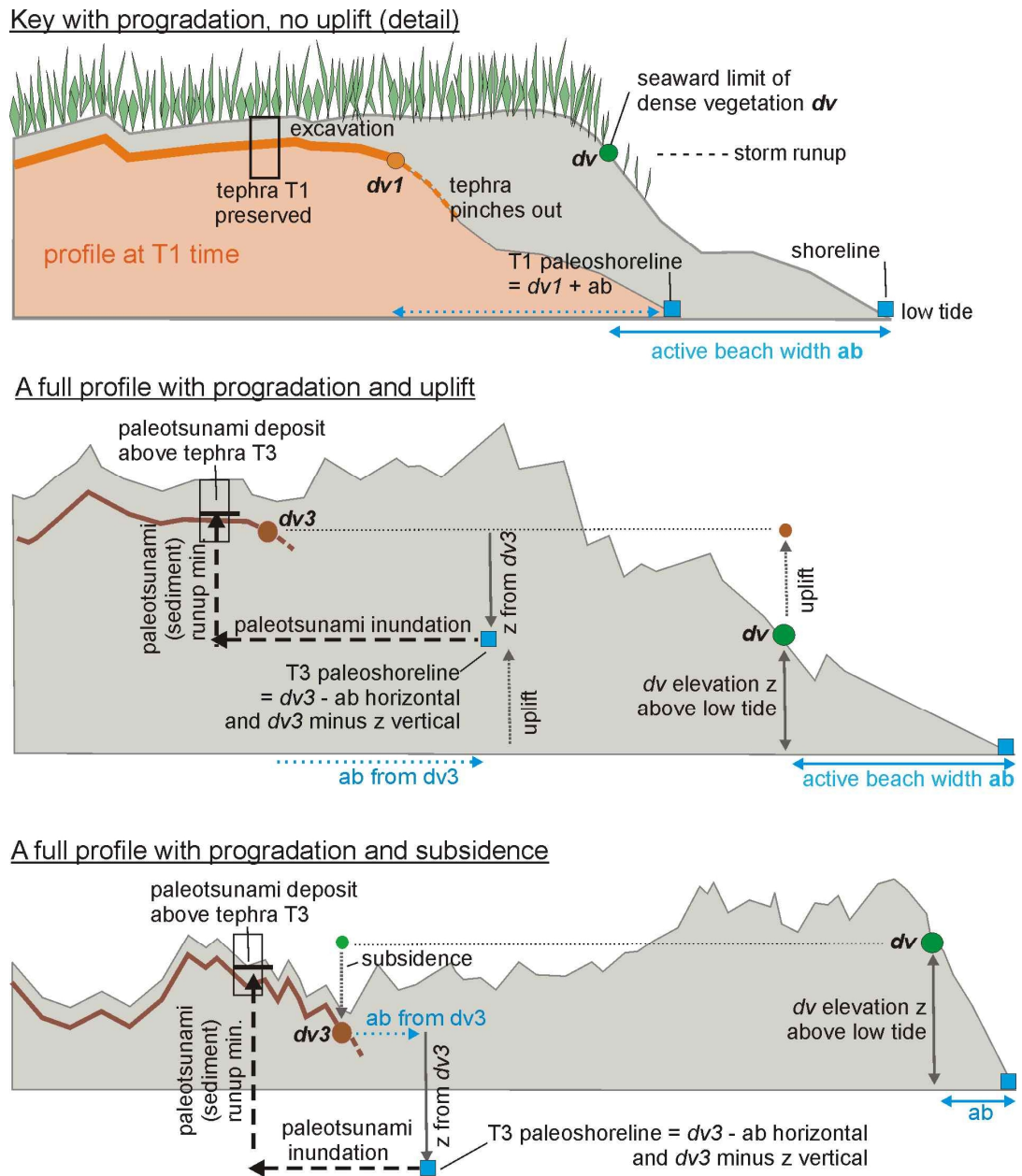
Figure S5. Idealized cartoons showing means for reconstructing paleoshorelines on profiles, using preserved tephra (as in Pinegina et al., 2013; MacInnes et al., 2016). The upper diagram is schematic of about 100 m width of shoreline (revised from Pinegina et al., 2013). The middle profile is based on Chazhma 220, about 350 m wide, maximum height about 8 m. The lower profile is from the Storozh 002, about 600 m wide, maximum height about 6 m. While these drawings are based on actual profiles, the illustrations are schematic and the tephra are not actual examples. Shorelines and their paleo-equivalents are shown as blue boxes in these 2-D views. The other primary reference point *dv* is the elevation above low tide of the first dense vegetation. The upper detail shows that it is near *dv* that tephra are preserved shoreward and not preserved seaward. From *dv* on any profile, we can measure down to low tide (vertical distance z) and seaward to the shoreline (horizontal distance ab). To reconstruct a paleoshoreline, we find a paleo *dv* and apply the modern metrics of elevation and distance from the shoreline to place a paleoshoreline point, from which we can use a tsunami deposits to estimate paleotsunami (sediment) inundation and runup. These shoreline reconstructions are made for each tephra interval, that is, we locate where a tephra such as tephra 3 pinches out, and all tsunami deposits above that tephra but below the overlying one are treated with the same approximation of paleoshoreline location.
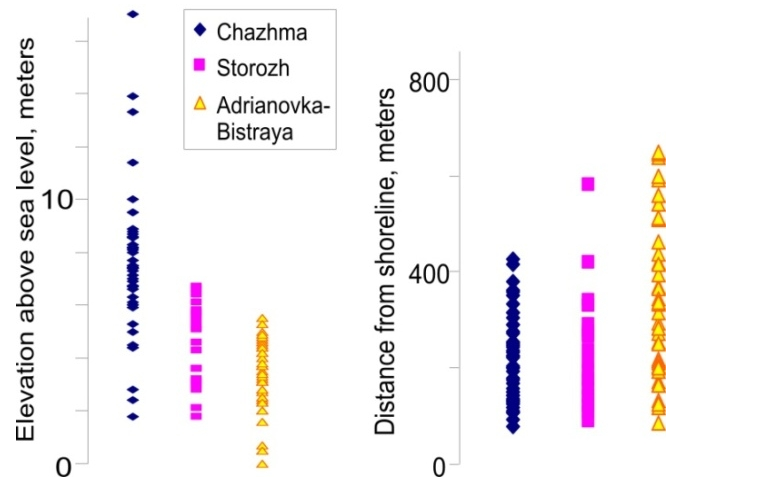
Figure S6. Distribution of elevations (meters above sea level) and distances (meters from modern shoreline) of excavations in the field area, southern Kamchatsky Bay, as originally compiled by Pinegina (2014). We use these distances and elevations for reconstructing tsunami sediment runup and inundation for 20th century tsunami deposits (Fig. S7). Note that the Chazhma area has higher elevations and narrower beach plains, and that the average elevations decrease northward (Chazhma to Bistraya), while the average beach plain width increases. In all, for example, there is only one excavation higher than 16 m, and only four excavations higher than 10 m. There are no excavations farther from the modern shoreline than about 600 m. Locations with symbols in Fig. S2.
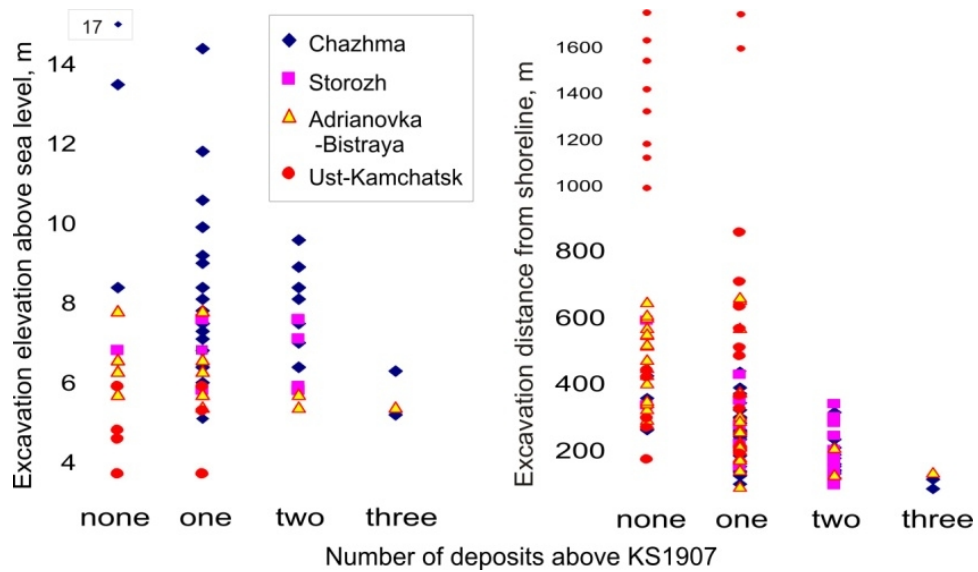
Figure S7. Elevation and distance of tsunami deposits above KS_{1907}, including data from the Ust' Kamchatsk area, north Kamchatsky Bay (Pinegina et al., 2012; Pinegina, 2014). In cases where there is only one deposit, it is the one not far stratigraphically above KS_{1907}, and thus which we interpret to have been deposited in 1923. This deposit reaches greater elevations and distances inland, being the largest 20th century tsunami in this bay. In cases where there are two deposits, the one in addition was at the surface in A.D. 2000 summer and is interpreted to be from the December 1997 Kronotsky tsunami. In a few excavations, there is a third, thin deposit between the other two, which we interpret to have been deposited by Chile 1960 tsunami (see Table S1). Locations with symbols in Figure S2.
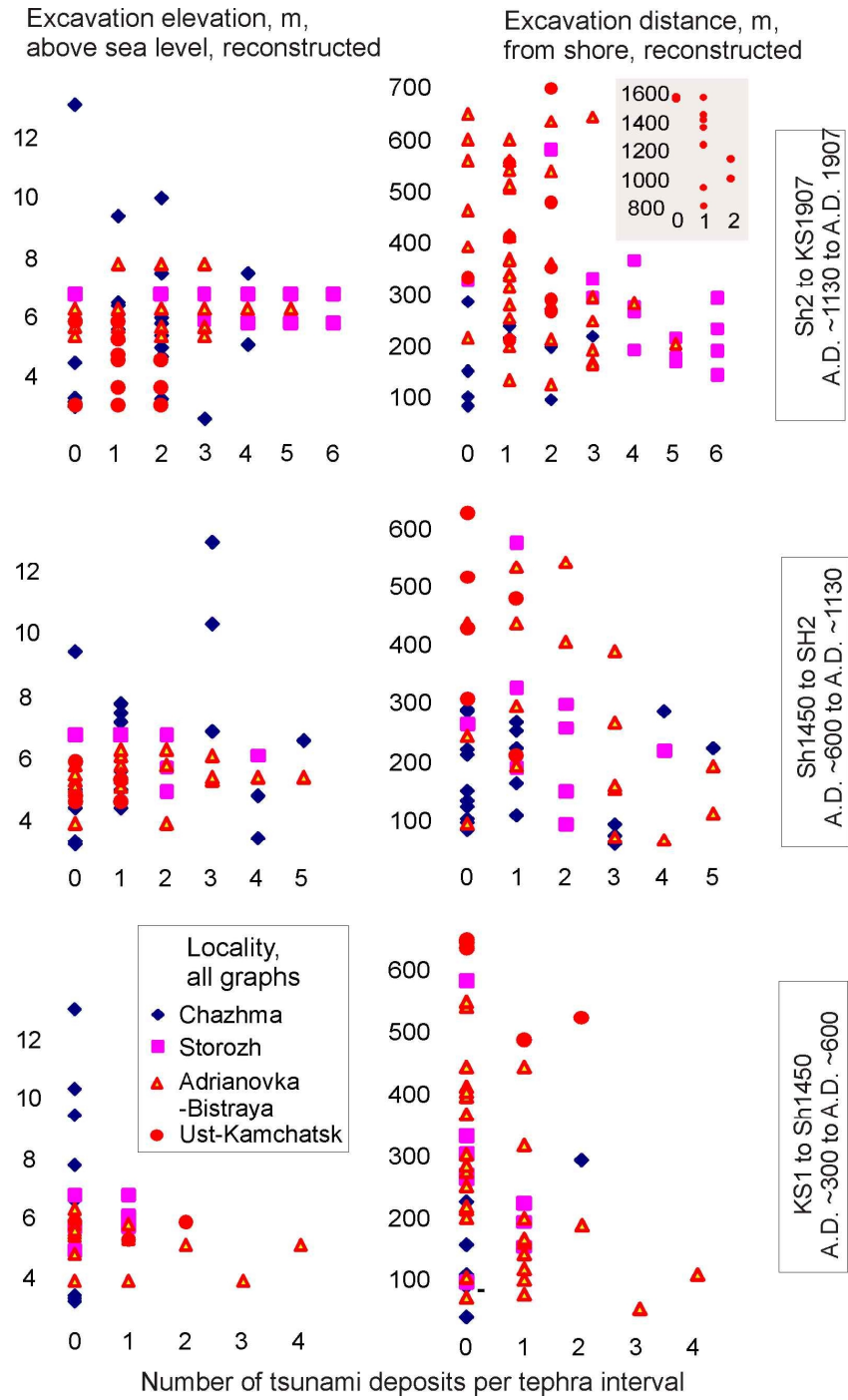
Figure S8. Number of paleotsunami deposits per tephra interval for three intervals below KS$_{1907}$ (for 20th century, see Fig, S7), including data from north Kamchatsky Bay near Ust-Kamchatsk (Pinegina et al., 2012; Pinegina, 2014). For each interval, the elevation and distance from shoreline of each excavation is reconstructed using methods as in Fig, S5. Locations with symbols in Fig. S2.
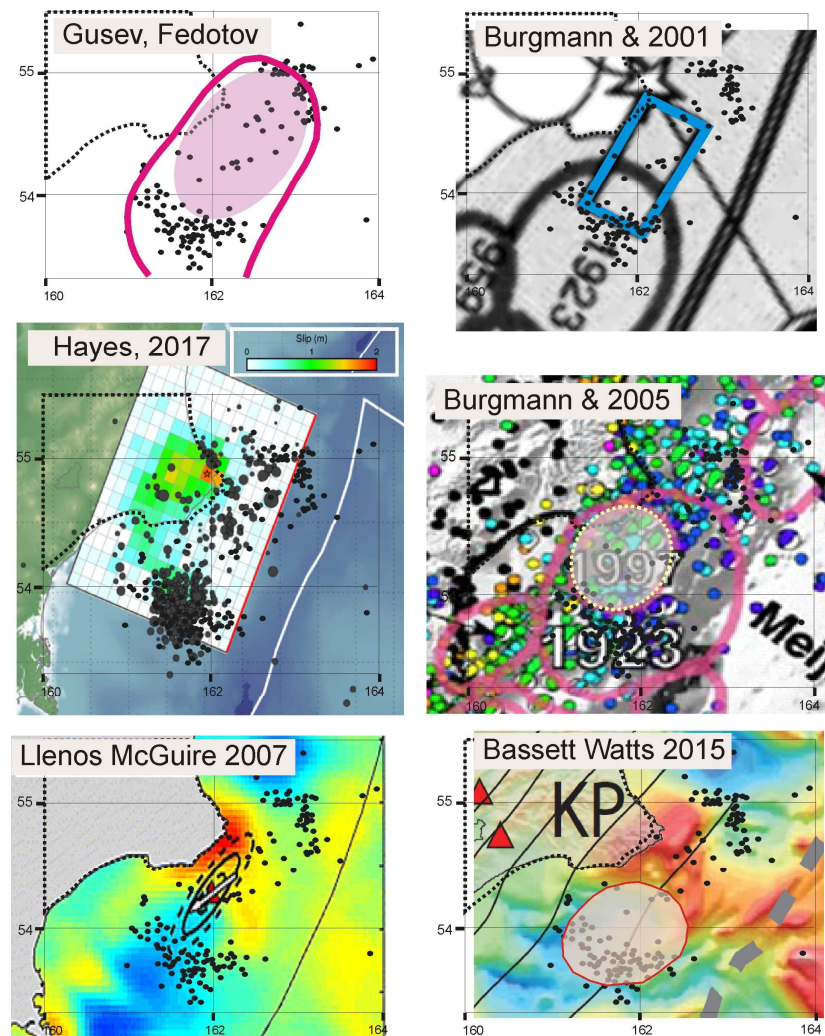
Figure S9. Rough comparison of rupture locations of the 5 December 1997 earthquake, all using the same base map with plotted aftershocks (traced from Gusev et al., 1998). Maps are scaled to the latitude and longitude of that base map (upper left) or fitted to the peninsula outline; because different map projections are used, this comparison is rough; maps are lined up vertically and horizontally. Not all symbols and scales are shown, only ones important to earthquake location and nature.

From upper left, counter-clockwise: **Gusev, Fedotov**: Gusev (2004) (Fig. S1) chose to outline the entire aftershock area as a rupture zone for the earthquake (dark pink outline), whereas Fedotov et al. (1998) did not draw an outline but interpreted that the earthquake filled a gap between the February and April 1923 events, which is approximated by the transparent pink ellipse. **Bürgmann et al. 2001**: Based on their dislocation model *Bcos* based on GPS measurements; rectangle is surface projection of the model fault. **Bürgmann et al. 2005**: [background is instrumentally recorded seismicity]; original figure caption states: "Bold red outlines labeled with year are the rupture zones of large historic earthquakes determined from aftershock distributions [Johnson and Satake, 1999]"; however, that 1999 reference does not mention or plot the 1997 Kronotsky earthquake, and the rupture zones are from Fedotov et al. 1982, from which Johnson and Satake omit the April 1923 event and misplot 1917 (to the north of this map zone). **Bassett and Watts 2015:** Ellipse (superimposed trace) is identified as "Coseismic slip/aftershock zone…" of the 1997 Kronotsky earthquake "modified from Bürgmann et al [2005]" Background is residual bathymetry, the positive features associated with the Emperor Seamount chain impinging on Kronotsky Peninsula (KP). **Llenos and McGuire 2007**: Characteristic rupture ellipses for the 1997 Kronotsky earthquake with major axes of length 0.5 Lc (inner dashed ellipse), 1 Lc (solid black ellipse) and 1.5 Lc (outer dashed ellipse) (Lc is characteristic rupture length) plotted on a TPGA (trench-parallel gravity anomaly) map; rupture directivity (arrow), centroid location (triangle); thin black line is trench axis. **Hayes 2017** (also see https://earthquake.usgs.gov/earthquakes/eventpage/usp0008btk#finite-fault): from finite fault modeling: Surface projection of modeled 1997 slip distribution superimposed on GEBCO bathymetry; modeling used a hypocenter matching or adjusted slightly from the initial NEIC solution (Lon. = 162.0 deg.; Lat. = 54.8 deg., Dep. = 34.0 km), and a fault plane defined using either the rapid W-Phase moment tensor (for near-real time solutions), or the gCMT moment tensor (for historic solutions). White line: plate boundary, gray circles are aftershock locations (up to 7 days), sized by magnitude.

References for supplementary material

Bassett, D. and Watts, A. B.: Gravity anomalies, crustal structure, and seismicity at subduction zones: 1. Seafloor roughness and subducting relief, Geochemistry, Geophysics, Geosystems, 16, 1508-1540, doi/10.1002/2014GC005684, 2015.

Bürgmann, R., Kogan, M.G., Levin, V.E., Scholz, C.H., King, R.W. and Steblov, G.M.: Rapid aseismic moment release following the 5 December, 1997 Kronotsky, Kamchatka, earthquake, Geophys. Res. Lett., 28, 1331-1334, doi: 10.1029/2000GL012350, 2001.

Bürgmann, R., Kogan, M.G., Steblov, G.M., Hilley, G., Levin, V.E. and Apel, E.: Interseismic coupling and asperity distribution along the Kamchatka subduction zone, J. Geophys. Res., 110, B07405, doi/10.1029/2005JB003648, 2005.

Engdahl, E. R., Villasenor, A.: Global seismicity: 1900-1999: in W.H.K. Lee, H. Kanamori, P.C. Jennings and C. Kisslinger, eds., International Handbook of Earthquake and Engineering Seismology, Part A, Ch. 41, 2002, 665-690. Academic Press. Accessed online Feb 2010. http://earthquake.usugs.gov/research/data/centennial.php

Fedotov, S.A., Chernyshev, S.D., Matviyenko, Y.D., and Zharinov, N.A.: Prediction of Kronotskoye earthquake of December 5, 1997, M = 7.8-7.9, Kamchatka, and its strong aftershocks with M > or = 6, Volcanology and Seismology, 6, 3-16, 1998, [in Russian].

Gusev, A. A.: The schematic map of the source zones of large Kamchatka earthquakes of the instrumental epoch: in Complex seismological and geophysical researches of Kamchatka. To 25th Anniversary of Kamchatkan Experimental & Methodical Seismological Department^ Ed. by E.I. Gordeev,V.N. Chebrov. Petropavlovsk-Kamchatsky, 445 pp., 2004 [in Russian].

Gusev, A. A., Levina, V. I., Saltykov, V. A., Gordeev, E .I.: Large Kronotskoye earthquake of Dec. 5, 1997: basic data, seismicity of the epicentral zone, source mechanism, macroseismic effects: in Gordeev et al., eds., 32-54, 1998 [In Russian with English abstract and figure captions].

Gusev, A. A., Shumilina, L. S.: Recurrence of Kamchatka strong earthquakes on a scale of moment magnitudes: Izvestiya, Physics of the Solid Earth, 40, 206-215, 2004.

Hayes, Gavin P.: The finite, kinematic rupture properties of great-sized earthquakes since 1990, Earth and Planetary Science Letters, 468, 94-100, doi: https://doi.org/10.1016/j.epsl.2017.04.003, 2017.

Llenos, A. L., and McGuire, J. J.: Influence of fore arc structure on the extent of great subduction zone earthquakes, Journal of Geophysical Research: Solid Earth, 112, B09301, doi:10.1029/2007JB004944, 2007.

Luneva, M. N., Lee, J. M.: Shear wave splitting beneath South Kamchatka during the 3-year period associated with the 1997 Kronotsky earthquake, Tectonophysics, 374, 135-161, doi:10.1134/S1819714016040059, 2003.

NCEI, National Centers for Environmental Information (formerly NGDC), Natural Hazards Data, Images and Education, Tsunami and Earthquake databases: https://www.ngdc.noaa.gov/hazard/hazards.shtml

MacInnes, B., Kravchunovskaya, E., Pinegina, T., Bourgeois, J.: Paleotsunamis from the central Kuril Islands segment of the Japan-Kuril-Kamchatka subduction zone, Quaternary Research, 86, 54–66, https://doi.org/10.1016/j.yqres.2016.03.005, 2016.

Pinegina T. K.: Time-space distribution of tsunamigenic earthquakes along the Pacific and Bering coasts of Kamchatka: insight from paleotsunami deposits, Doctor of Geological Science dissertation, Institute of Oceanology RAS, Moscow, 235 pp., 2014 [in Russian].

Pinegina, T. K., Bazanova, L. I.: New data on characteristics of historical tsunamis on the coast of Avacha Bay (Kamchatka), Bulletin of Kamchatka regional association "Educational-scientific center". Earth sciences, 3, 5-17, 2016 [in Russian with English abstract].

Pinegina, T.K., Bourgeois, J., Bazanova, L.I., Melekestsev, I.V., and Braitseva, O.A.: A millennial-scale record of Holocene tsunamis on the Kronotsky Bay coast, Kamchatka, Russia, Quaternary Res., 59, 36-47, DOI: https://doi.org/10.1016/S0033-5894(02)00009-1, 2003

Pinegina, T.,K., Bourgeois, J., Kravchunovskaya, E. A., Lander, A.V., Arcos, M. E., Pedoja, K. and MacInnes B.T.: A nexus of plate interaction: Vertical deformation of Holocene wave-built terraces on the Kamchatsky Peninsula (Kamchatka, Russia), Geological Society of America Bulletin , 125, 1554-1568, doi: 10.1130/B30793.1, 2013.

Pinegina, T. K., Kozhurin, A. I., Ponomareva, V. V.: Seismic and tsunami hazard assessment for Ust-Kamchatsk settlement, Kamchatka, based on paleoseismological data, Bulletin of Kamchatka regional association "Educational-scientific center". Earth sciences. 1, 138-159, 2012 [in Russian with English abstract].

Pinegina, T. K., Kozhurin, A. I., Ponomareva, V. V.: Active Tectonics and Geomorphology of the Kamchatsky Bay Coast in Kamchatka, Russian Journal of Pacific Geology, 8, 65–76, 10.1134/S1819714014010047, 2014.

Slavina, L. B., Pivovarova, N. B., Levina, V. I.: A study in the velocity structure of December 5, 1997, Mw = 7.8 Kronotskii rupture zone, Kamchatka, J. Volcanology & Seismology, 1, 254-262, doi:10.1134/S0742046307040045, 2007.

Sohn, S.W.: The 1997 Kamchatka earthquake. Individual Studies by Participants at the International Institute of Seismology and Earthquake Engineering, 34, 91-99, 1998. PB: International Institute of Seismology and Earthquake Engineering.

Zayakin, Yu. A., Luchinina, A.A.: Catalogue tsunamis on Kamchatka, Obninsk: VNIIGMI-MTSD, 51pp., 1987 [Booklet in Russian].

Zobin, V. M., Levina, V. I.: The rupture process of the Mw 7.8 Cape Kronotsky, Kamchatka, earthquake of 5 December 1997 and its relationship to foreshocks and aftershocks, Bull. Seis. Soc. Am., 91, 1619-1628, doi: 10.1785/0119990116, 2001.